Tsunami Hazard Assessment of the Elementary School Berm Site in Long Beach, WA

Frank González, Randy LeVeque and Loyce Adams

University of Washington

1 Background

The probability that an earthquake of magnitude 8 or greater will occur on the Cascadia Subduction Zone (CSZ) in the next 50 years has been estimated to be 10-14% (Petersen, et al., 2002). The last such event occurred in 1700 (Satake, et al., 2003; Atwater, et al., 2005) and future events are expected to generate a destructive tsunami that will inundate Long Beach and other Washington Pacific coast communities within tens of minutes after the earthquake main shock.

As a result of the Project Safe Haven planning process, the Long Beach School District proposed the construction of a vertical evacuation berm behind the Long Beach Elementary School (Project Safe Haven, 2011a). Consequently, the Washington Emergency Management Division funded this study to assess the tsunami hazard at the proposed berm site. This report presents estimates, based on GeoClaw tsunami inundation model results, of the maximum flooding and current speeds at the berm site for two earthquake scenarios, a magnitude 9.2 (9.2M) event on the Alaska Aleutian Subduction Zone (AASZ) and a 9M event on the Cascadia Subduction Zone (CSZ).

2 Earthquake Scenarios

In the general context of tsunami hazard assessment and emergency management planning, there are two general classes of tsunamigenic earthquake scenarios that represent quite different threats. A *distant*, or *far-field*, earthquake generates a tsunami that must traverse the open ocean for hours, generally losing a significant percentage of the destructive energy it had in the generation zone. In contrast, a *local*, or *near-field*, earthquake generates a tsunami that arrives at a nearby community in tens of minutes with much smaller loss of energy during the short propagation distance from the generation zone. This study considers a tsunamigenic earthquake scenario of each type.

The *local* or *near*-field M9 earthquake on the CSZ simulated in this study is the L1 scenario developed by Witter, et al (2011); it is one of 15 seismic scenarios used in a hazard assessment study of Bandon, OR, based on an analysis of data spanning 10,000 years. There is significant uncertainty in assigning an average return period to the L1 scenario, but based on a simple analysis of the evidence presented by Witter et al. (2011) on the estimated ages of M9 and larger CSZ earthquakes, a range of 1990-3300 years seems reasonable (R. Witter, personal communication). The length and width of L1 are approximately 1000 km and 85 km, respectively; salient features of the earthquake crustal deformation include coastal subsidence at Long Beach of about 1-2 m and a zone of about 8 to 10 m maximum uplift about 75 km offshore (Figure 1). This L1 scenario was chosen by WA DNR because the resulting inundation line is interpreted as the 95% confidence level that the inundation will not be exceeded (Witter et al., 2011).

The distant or far-field M9.2 earthquake on the AASZ simulated for this study is similar to the 1964 Alaska event, which was the second largest worldwide since about 1900, when earthquake recordings began. The associated tsunami caused tremendous loss of life and property in Alaska and Crescent City, CA. This same scenario was developed and used in a previous study of Seaside, OR (Gonzalez, et al., 2009) and was also included in the Witter, et al. (2011) study of Bandon, OR. The Tsunami Pilot Study Working Group (TPSWG, 2006) estimated the mean return period of this scenario to be about 750 years.

This scenario was chosen by WA DNR because, of all historic events, the 1964 Alaska tsunami had the most destructive impact on the Northwest coast.

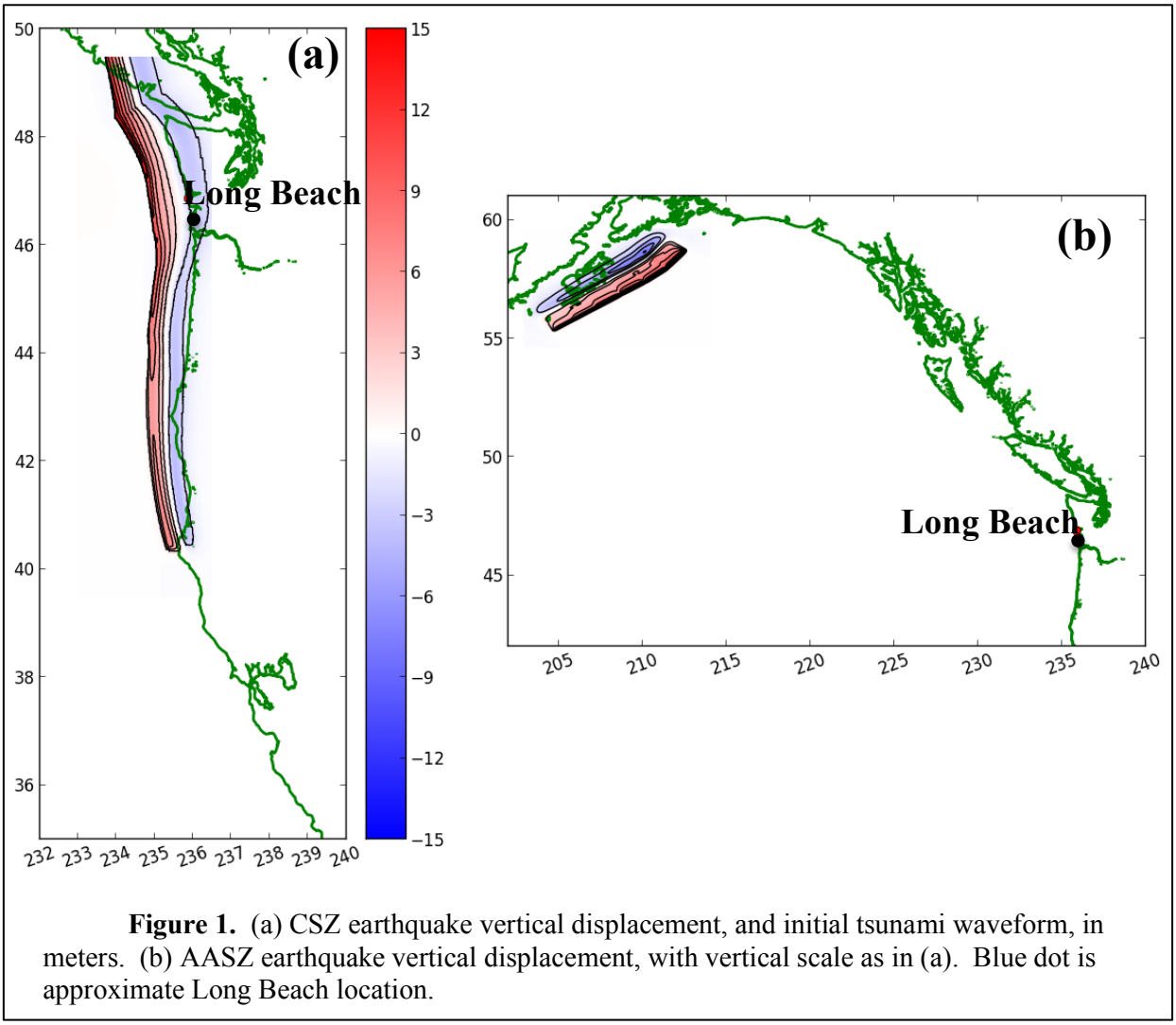

Figure 1. (a) CSZ earthquake vertical displacement, and initial tsunami waveform, in meters. (b) AASZ earthquake vertical displacement, with vertical scale as in (a). Blue dot is approximate Long Beach location.

3 Tsunami Modeling Results

The simulations of tsunami generation, propagation and inundation were conducted with the GeoClaw model. The GeoClaw model solves the nonlinear shallow water equations, has undergone extensive verification and validation (LeVeque and George, 2007; LeVeque, et al., 2011) and has been accepted as a validated model by the U.S. National Tsunami Hazard Mitigation Program (NTHMP) after conducting multiple benchmark tests as part of an NTHMP benchmarking workshop (NTHMP, 2012).

Computational grids for the AASZ used the 1/3 arc-second Digital Elevation Model (DEM) known as "Astoria V2" (Love, et al., 2012) downloaded from the NOAA/NGDC website http://www.ngdc.noaa.gov/dem/squareCellGrid/download/4090 . These data were adequate for the AASZ scenario, since inundation was restricted to a narrow strip of beach (see Section 3.1). To ensure the best quality "bare earth" topographic DEM, a decision was made to develop a DEM using 1-m spatial resolution Lidar data collected by Watershed Sciences for the Oregon Department of Geology and Mineral Industries (DOGAMI) in 2009 (DOGAMI, 2010). Subsequently, Washington DNR developed the 1/3-arc-second DEM from the Lidar data (Figure 2) and provided it to the authors of this

study (S. Slaughter and T. Walsh, personal communication); a vertical datum adjustment was required to integrate the Lidar DEM into the Astoria V2 DEM, and this adjustment was reviewed by an NGDC DEM development expert (B. Eakins, personal communication). In order to adequately represent the topography in the berm site, this Lidar DEM was interpolated to 1/6 arc-sec for the numerical computations, corresponding to linear dimensions of approximately 3.5m x 5m in the East-West and North-South directions, respectively; output values on the fixed inundation grid were further interpolated to 1/12 arc-second. All simulations were conducted with the tide level set to Mean High Water (MHW), which is standard practice for studies of this type.

We next present results for three simulations: the AASZ scenario; the CSZ Bare Earth scenario, i.e., without the berm DEM; the CSZ Berm scenario, with the berm DEM.

Figure 2. Google Earth image of the Long Beach area. The yellow lines mark the geographical extent of the 1/3 arc-second DEM developed for this study by WA DNR, using the 1-m resolution Lidar data collected for DOGAMI in 2009 (DOGAMI, 2010), and the yellow bulls-eye symbol marks the location of the proposed berm.

3.1 AASZ Scenario

Figure 3 was obtained by storing the maximum computed flood depth (i.e., the depth of water above the local ground level) computed in each grid cell during the entire tsunami simulation. This scenario only produces flooding that is restricted to a narrow strip of the beach, with essentially no flooding of the residential areas to the east, including the proposed berm site. Because no flooding occurs at the berm

site, this scenario apparently poses no hazard and, in the following sections we concentrate on the results of the near-field CSZ M9 scenario.

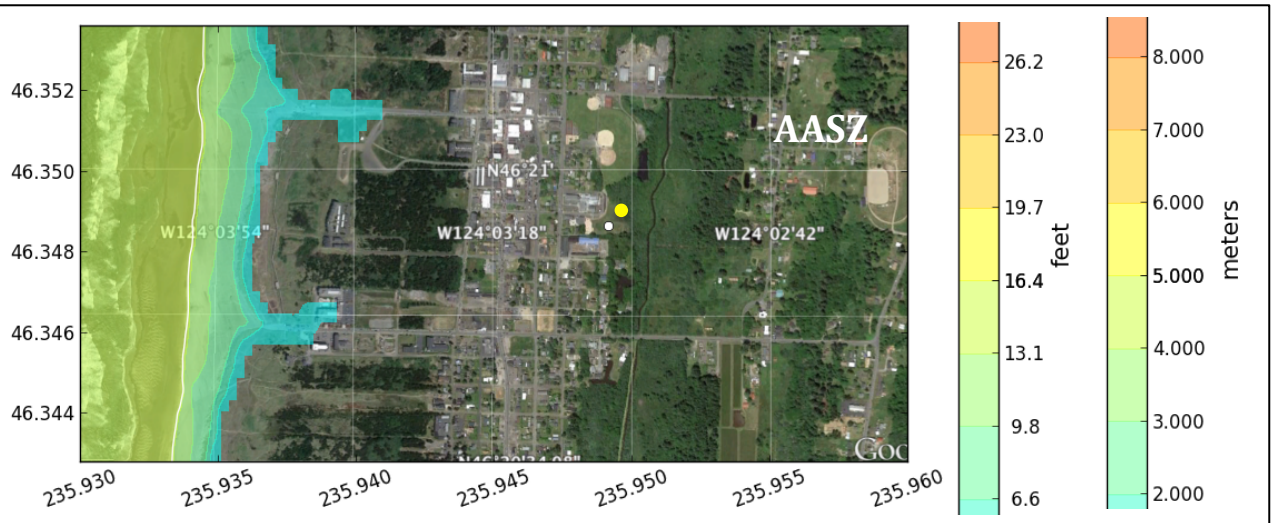

Figure 3. Maximum flood depth at Long Beach for the M9.2 AASZ scenario. Note the absence of flooding at the proposed berm site, east of the downtown area (yellow dot).

3.2 CSZ Scenarios

Here we present results for the near-field CSZ M9 event, known as L1. Two cases were simulated, each differing only by the absence or presence of a DEM representative of the berm topography, which we will refer to as the Bare Earth and Berm simulations, respectively.

Berm Digital Elevation Model

A berm DEM was developed by digitization of the topographic contours in the architectural drawing of the berm, Figure 1 of Project Safe Haven (2011b), and interpolation to a uniform (longitude, latitude) grid. This DEM is an approximation to the original Berm design; the lower half of the drawing was digitized, then flipped to create the upper half, resulting in a structure that is symmetric about its east-west axis. Non-symmetric deviations from the original design are small, so that the symmetric DEM is an approximation that captures the primary features of the tsunami/berm interaction with a fidelity that is adequate for the main purpose of this study – namely, to determine whether or not a tsunami generated by the L1 CSZ event is likely to overtop the berm.

Figure 4 (a) superimposes the berm DEM on a Google Earth image of the Long Beach Elementary School campus. The maximum height of the berm structure is 6.1 m (20 ft) above the base, and the base is situated on bare ground that is 2.7 m above local MHW, the vertical reference level ("zero level") of the numerical model, so that the top of the berm is at a height of 8.8 m, relative to local MHW. This berm geometry is illustrated by the blue line in Figure 4 (b), an East-West transect through the berm before the earthquake and the associated subsidence of the berm site occurs.

Co-seismic Subsidence

Subduction zone earthquakes are typically accompanied by co-seismic uplift seaward and subsidence landward. This pattern is clearly seen in the vertical displacement for the CSZ event presented in Figure 1 (a). During this event, subsidence occurs over the entire Long Beach peninsula and, in particular, the ground subsides by approximately 2 m at the Long Beach berm site. This subsidence results in an

associated drop in the elevation of the top of the berm from 8.8 m to 6.8 m above MHW, as shown by the green transect line in Figure 4 (b).

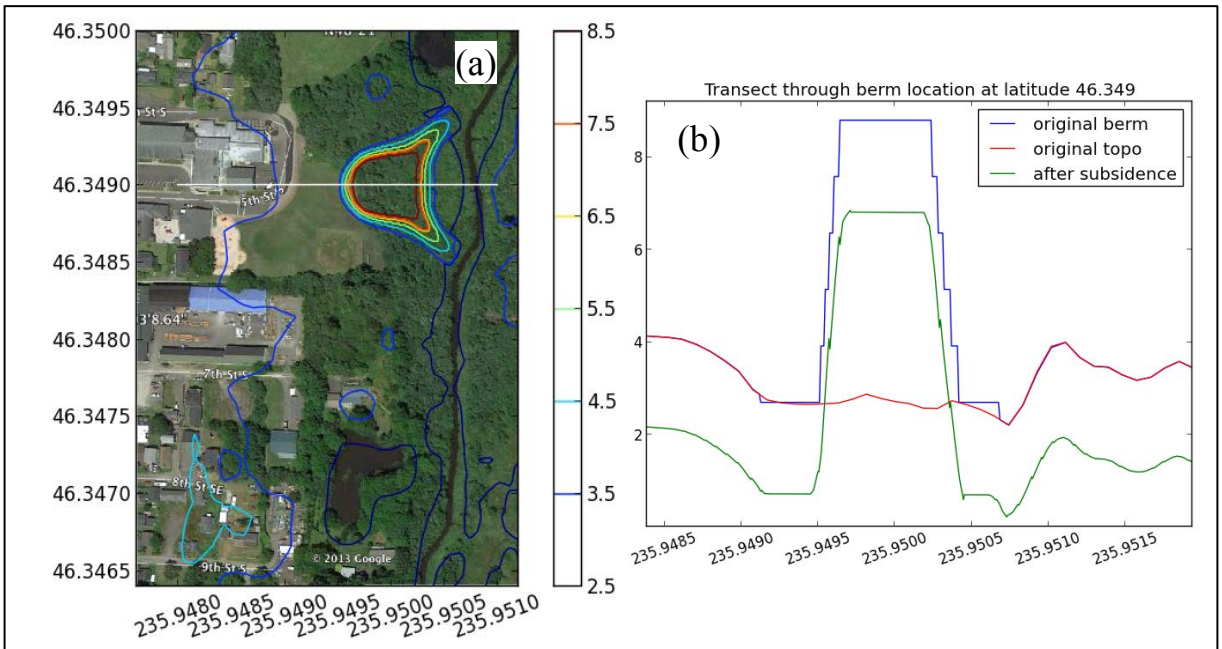

Figure 4. Digital elevation model of the berm. (a) Elevation contours superimposed on Google Earth image of Long Beach Elementary School campus. School buildings are directly west of the berm. (b) East-West transect through the berm before and after the earthquake main shock and the associated subsidence of approximately 2 m.

Maximum Flooding Depth

In contrast to the AASZ scenario, the CSZ Bare Earth event tsunami sweeps across the entire Long Beach peninsula (Figure 5); flood depths in excess of 5 m extend eastward from the Pacific coast, through residential and downtown Long Beach, gradually decreasing to a depth of about 1-3 m on the Willapa Bay shoreline.

Figure 6 presents the time series of flooding depth at the berm site. There are a number of interesting features that bear on the overall nature and temporal evolution of the flood. The overall shape is that of a single wave over the 42 minute duration of the simulation (later waves might reach the berm site, but their amplitude would likely be much smaller). The wave front arrives at the berm position 28 minutes after the earthquake main shock, rises rapidly over the next 2 minutes to a peak value of 4.4 m at 30 minutes after the main shock, then decreases more slowly over the next 12 minutes to a value of 2.3 m.

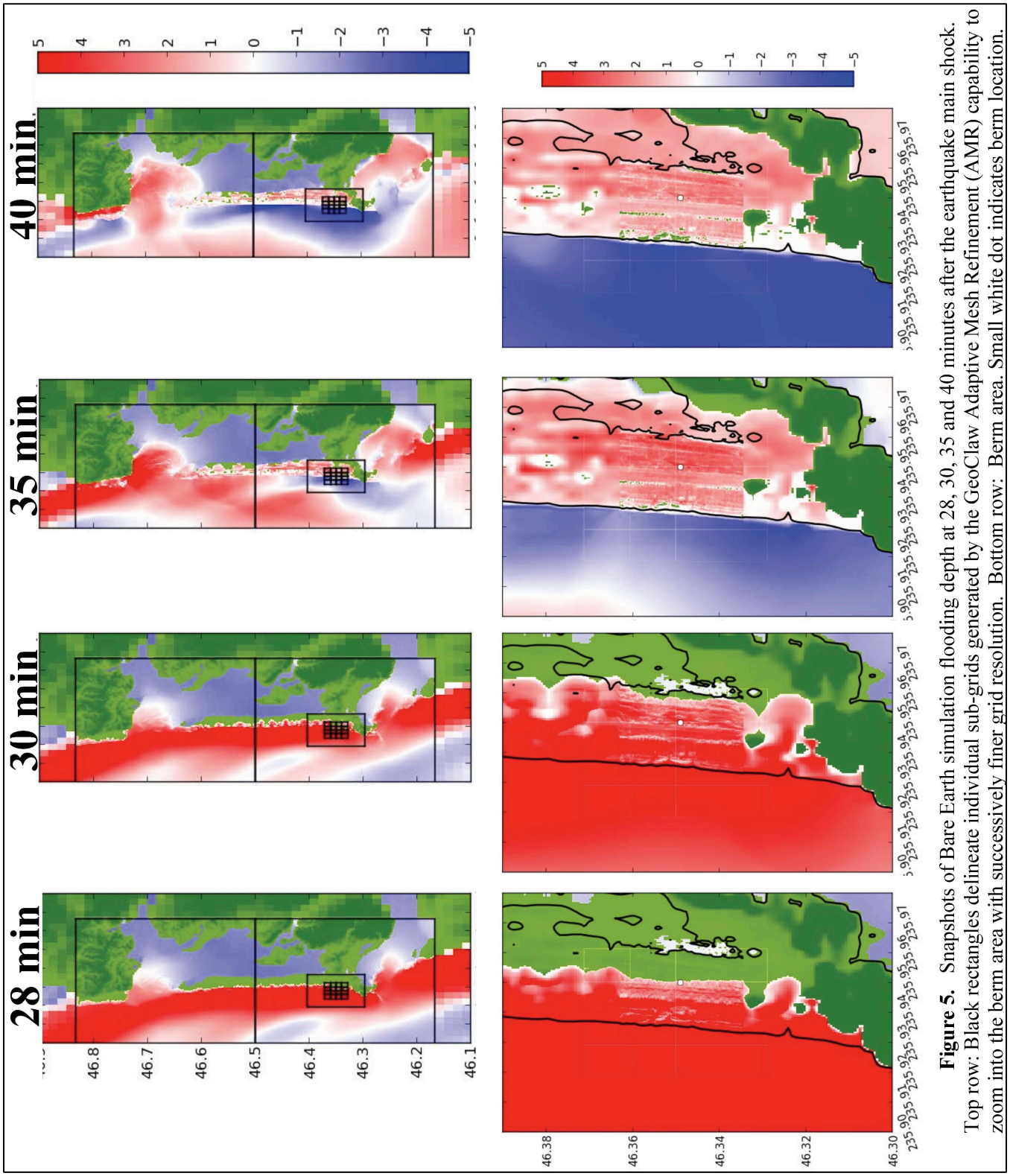

Figure 5. Snapshots of Bare Earth simulation flooding depth at 28, 30, 35 and 40 minutes after the earthquake main shock. Top row: Black rectangles delineate individual sub-grids generated by the GeoClaw Adaptive Mesh Refinement (AMR) capability to zoom into the berm area with successively finer grid resolution. Bottom row: Berm area. Small white dot indicates berm location.

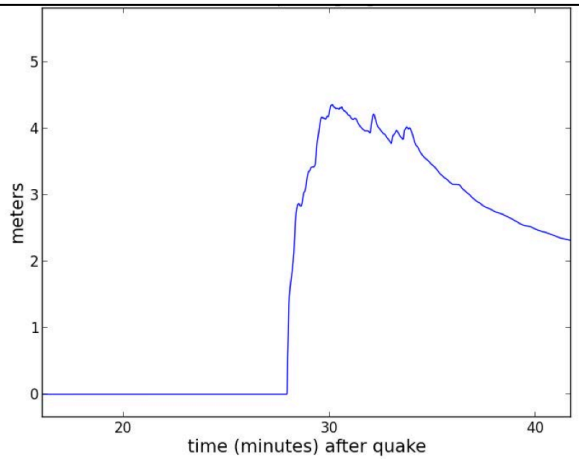

Figure 6. Bare Earth flood depth time series at the berm site.

Figure 7 presents maps of maximum flood depth for both the Bare Earth and Berm simulations in a small area that encompasses both the proposed berm and the major buildings of the Long Beach Elementary School campus. The maximum flood depth at (bare earth) locations of campus buildings is in the range of 3-4 m (10 – 13 ft), so that single story structures are likely to be overtopped; this is most easily seen in the top pair of maps in Figure 7, which are superimposed on a Google Earth image of the school campus. The flood depth pattern is perturbed near the berm, with higher values upstream (west) of the berm and lower values downstream (east) of the berm; however, at distances greater than a "characteristic berm length" of about 100 m the flood depth pattern is very similar in both simulations. This is most easily seen in the bottom pair of maps in Figure 7.

Transects of maximum flood depth were constructed through a reference point on the berm, oriented North-South and East-West (Figure 8). Here, the near-berm differences in maximum flood depth between the Bare Earth and Berm simulations are more apparent. (In Figure 8, a plotting artifact associated with a linear extrapolation artificially increases the flooding depth on the surface of the berm, and these values at the berm are therefore ignored in what follows.) The top pair of transects in Figure 8 present the upstream and downstream differences along the berm East-West axis. Relative to the Bare Earth flooding depth, the corresponding depth at the upstream face of the berm increases by 1.2 m, rising to within 60 cm of the top of the berm; at the downstream surface of the berm, the flooding depth decreases by about 40 cm to a value 2.2 m below the top of the berm. The bottom pair of transects in Figure 8 present the differences in flooding depth at two points on the North and South sides of the berm; in each case, flooding depth increases by about 30 cm, rising to within 1.5 m of the berm top.

Maximum Current Speed

Strong currents can be highly dangerous, demolishing structures and transporting logs, boats, automobiles and other rolling stock to form fields of debris that act as battering rams to multiply the destructive impact of the tsunami. Figure 9 presents maximum current speed maps in the berm area. The spatial patterns are complex, with typical values of 6-8 m/s but they include areas with values as low as 2 m/s and as high as 10 m/s. Bare Earth flow speeds at the berm site are 5-6 m/s, but the Berm simulation is characterized by a local minimum that encircles the berm with a value of about 1 m/s. This minimum is a reflection of the model boundary conditions, which prohibit flow through the berm by requiring that the velocity normal to a berm surface is zero, a physically reasonable condition.

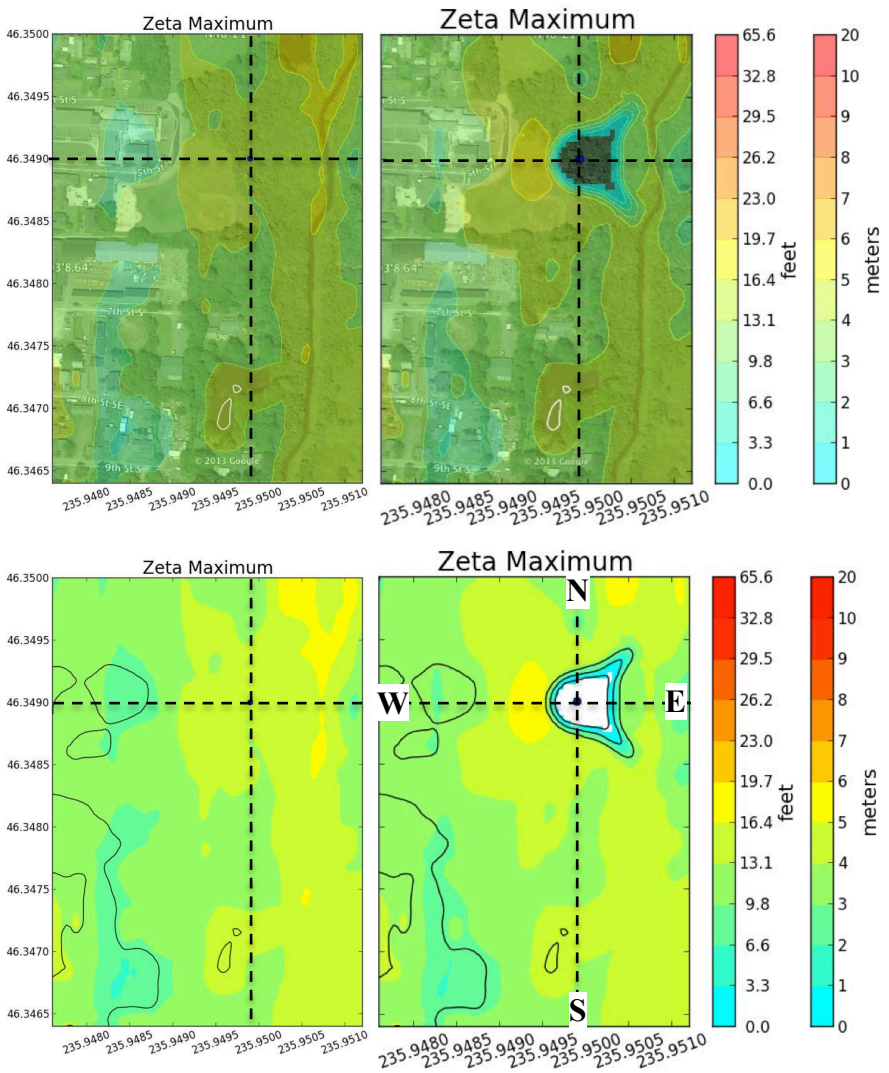

Figure 7. Maximum flooding depth for CSZ scenarios. Left pair: Bare Earth simulation. Right pair: Berm simulation. The top pair of maps are superimposed on Google Earth images. Dashed lines are East-West and North-South transects through a reference point on the berm with coordinates (235.9499 deg East, 46.3490 deg North), as annotated on lower right map.

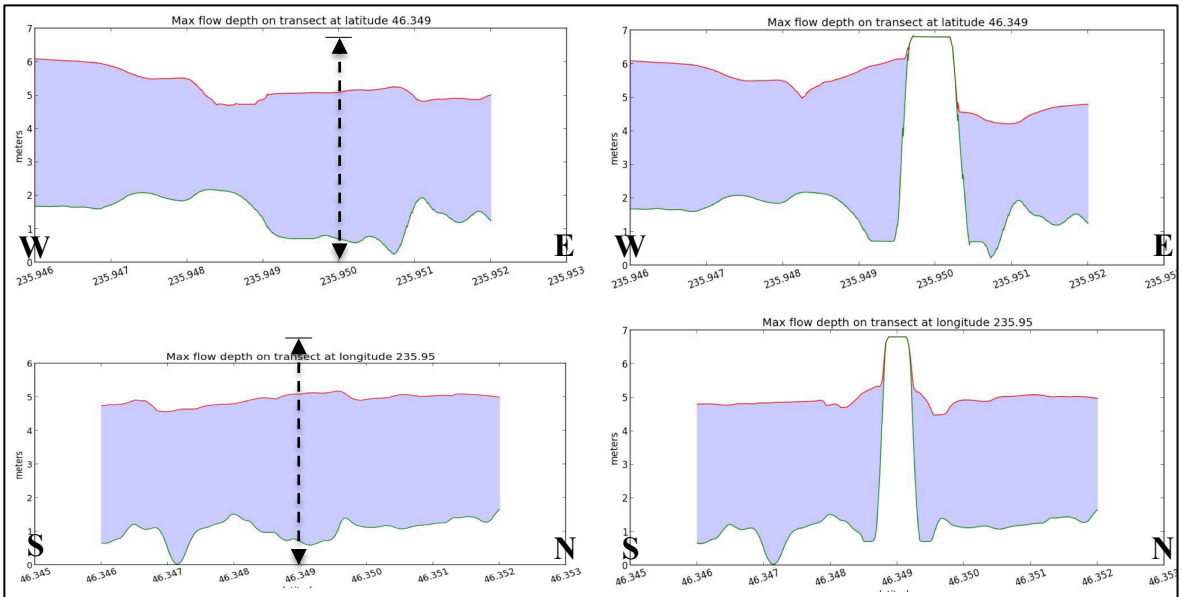

Figure 8. Transects of maximum flow depth taken through the berm reference point at (235.95 E, 46.349 N) and oriented North-South and East-West, as shown in Figure 7, bottom right map. Left pair are Bare Earth simulations; for reference, the location and height of the (absent) berm are indicated by the vertical arrows. Right pair are Berm simulations.

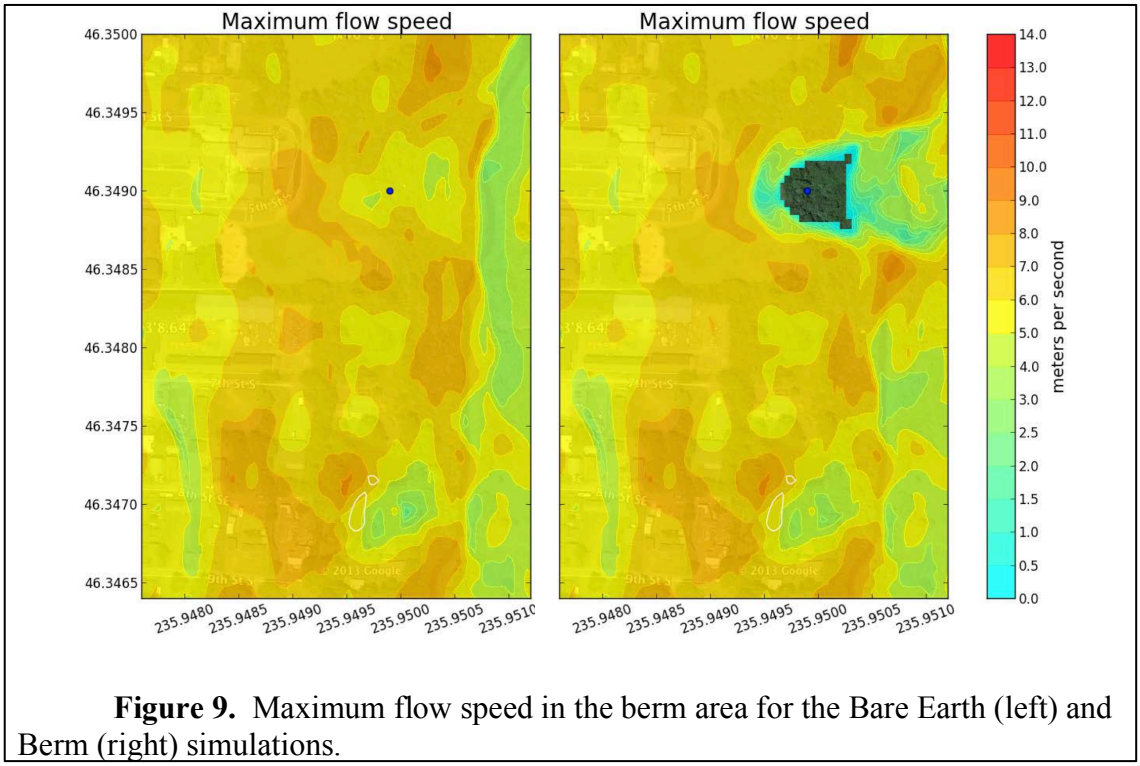

Figure 9. Maximum flow speed in the berm area for the Bare Earth (left) and Berm (right) simulations.

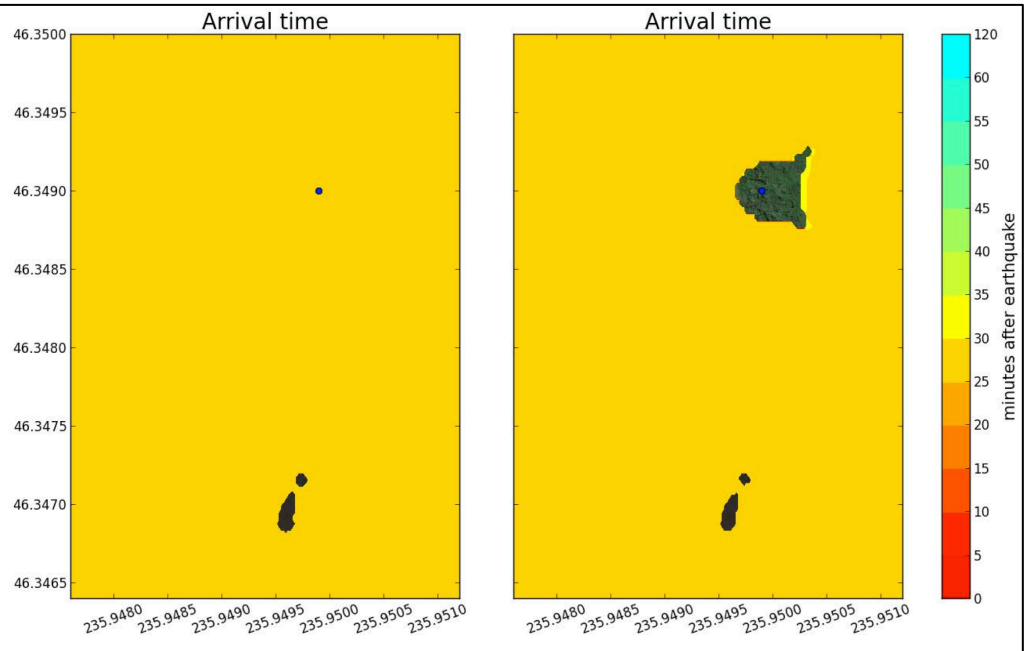

Figure 10. Arrival time after earthquake main shock for the Bare Earth simulation (left) and the Berm simulation (right).

Arrival Time

Figure 10 presents the tsunami arrival times, referred to the time of the earthquake main shock, for each scenario. The tsunami arrives at the coast in about 20 minutes (not shown) and reaches the berm site about 10 minutes later, i.e., about 30 minutes after the earthquake main shock.

4 Uncertainties and Limitations

Numerical models do not produce perfect simulations of any natural process. Here we discuss uncertainties and limitations most important to this specific study and, where possible, their probable influence on the model output.

4.1 Source Specification

This is likely the largest source of uncertainty in the study. Variations in the value of certain earthquake parameters can produce large differences in the subsequent tsunami flooding.

Earthquake Magnitude and Recurrence Interval

In general, the greater the earthquake magnitude, the larger the initial wave amplitude (but see the discussion of slip distribution uncertainty, below, for exceptions to this general rule). With regards to the CSZ event, however, larger events would be associated with larger recurrence intervals than the estimated 1990-3300 years (R. Witter, personal communication). In addition, Witter et al. (2011) estimate that "…the L1 scenario captures 95 percent of the hazard and more severe events are extremely unlikely."

The AASZ event is similar to a historic event, the 1964 Prince William Sound earthquake, and the magnitude was estimated from direct measurements. Such events are estimated to occur more frequently than great CSZ events, with a recurrence interval of about 750 years (TPSWG, 2006), but the threat to the Long Beach Elementary School campus from such great earthquakes is greatly mitigated by the large distance the tsunami must traverse to the site.

Earthquake Slip Distribution

The vertical displacement of the earth's crust presented in Figure 1 (a) is the direct result of a Pacific oceanic tectonic plate slipping (or subducting) beneath the North American continental plate, deforming both plates in the process. But the amount of slip is not distributed evenly on the common surface, known as the fault plane, where the two plates are in direct contact. There are patches on the fault plane, known as asperities, in which the two plates are more tightly locked by friction or protrusions of one plate into the other. But the relentless movement of the tectonic plates over decades and centuries continues to build up stress until the rock in the asperity region breaks and the plates slip past one another, releasing a local maxima of energy.

A significant amount of earthquake energy is released by the slip in asperities, which concentrates the energy in a relatively small patch. As a consequence, details of the slip distribution can make a significant difference in the initial amplitude of a tsunami; for example, if the slip is distributed evenly over the entire fault plane, then the initial tsunami amplitude will be about half the amplitude of a tsunami generated by slip distributed evenly over half of the fault plane. In particular, high slip values concentrated in an asperity region are associated with large values of vertical displacement of the ocean floor and a higher initial tsunami wave in the region.

Thus, the location of a coastal community relative to an asperity and the associated high wave region can have a direct effect on the severity of flooding in the community. When an earthquake is in the far-field, such as the AASZ scenario considered here, the earthquake resembles a point or line source and the details of the slip distribution are less important. However, details of the near-field slip distribution for the CSZ scenario L1 can strongly affect the degree of Long Beach inundation. For example, offshore of Long Beach there is a maxima of 10-12 m in crustal deformation and the initial tsunami waveform (Figure 1(a)); if this maxima was located closer to or farther from Long Beach, the inundation would likely increase or decrease, respectively. Similarly, if the concentration of slip (and therefore earthquake energy) resulted in a larger or smaller maximum value, then a corresponding increase or decrease in flooding would be expected. However, it is not possible to make a reliable prediction of slip distribution at this level of detail, and conducting numerical experiments to estimate the sensitivity of flooding to such changes is beyond the scope of this study.

Landslide sources

This study did not include modeling of local landslides that are triggered by earthquake shaking. The impact of tsunamis generated by landslides is restricted to the local generation area, so that this is not an important process in the case of a far-field event like the AASZ earthquake used in this study. However, submarine landslides offshore Long Beach could increase the severity of flooding.

4.2 Model Physics

Certain values were assumed for important geophysical parameters, and some physical processes were not included in the simulations; their potential effect on the modeling results are discussed below.

Tide Stage

The simulations were conducted with the background sea level set to MHW. This value is conservative, in the sense that the severity of inundation results is increased for higher background sea level. Larger tide levels do occasionally occur, but the assumption of MHW is standard practice in studies of this type.

Friction

Manning's coefficient of friction was set to 0.025, a standard value used in tsunami modeling that corresponds to gravelly earth. This choice of 0.025 is conservative, because the presence of trees,

structures and vegetation to the west of the Long Beach Elementary School campus would justify the use of a larger value, which would tend to reduce the inland flow.

Structures

Buildings were not included in the simulations. The presence of structures will alter tsunami flow patterns and generally impede inland flow. The lack of structures in the model is therefore a conservative feature, in that their inclusion would generally reduce inland penetration of the tsunami wave.

Debris

Large tsunamis inevitably create fields of debris that act as battering rams, multiplying the destructive impact. But this process also requires the expenditure of tsunami energy, which would tend to reduce the inland extent of the inundation.

Tsunami modification of bathymetry and topography

Severe scouring and deposition are known to occur during a tsunami, undermining structures and altering the flow pattern of the tsunami itself. Again, this movement of material requires an expenditure of tsunami energy that tends to reduce the inland extent of inundation.

Hydrodynamic Equations

It is not clear that the GeoClaw shallow water equations are adequate to model the interaction of the flow with a small scale, steep-walled feature such as a berm. Ideally, a 3-dimensional fluid model would be coupled to GeoClaw in order to more accurately model the response around the berm. Such an effort was beyond the scope of this study.

5 Discussion and Summary

The AASZ tsunami produces only beach area flooding (Figure 3), and does not appear to pose a hazard to the berm site. The CSZ tsunami flooding does not overtop the berm, but rises to less than a meter below the berm top; furthermore, strong currents, in excess of 6 m/s, flow throughout the berm area. In this regard, we note again that the complex physical processes of wave/structure interaction, debris flow, scouring and deposition were not included in the model. These processes draw energy from the tsunami, so we expect that the inland penetration of flooding would be reduced; however, should flooding reach the berm, these processes will subject the structure to significant scouring and battering by debris fields. An improved simulation would include structures and the interaction of the tsunami with these structures; such a simulation, however, is beyond the scope of this study.

The values chosen for the background sea level and Mannings coefficient of friction result in a tendency to overestimate the severity of flooding. However, the effect of uncertainty associated with the details of CSZ earthquake characteristics, especially the details of the seismic slip distribution, is unknown. Since numerical experiments were not conducted to estimate the sensitivity of the berm site flooding to these source uncertainties, it is not possible to completely rule out a future CSZ earthquake with a different slip distribution that would increase or decrease the flooding depth at the berm site.

References

Atwater, Brian F, Musumi-Rokkaku Satoko, Kenji Satake, Tsuji Yoshinobu, Ueda Kazue, and David K Yamaguchi (2005): USGS Professional Paper 1707, pp 1–144.

Gonzalez, F I, E L Geist, B Jaffe, U Kânoğlu, H Mofjeld, C E Synolakis, V V Titov, et al. (2009): Probabilistic Tsunami Hazard Assessment at Seaside, Oregon, for Near- and Far-Field Seismic Sources, *Journal of Geophysical Research* 114 (C11) (November 24). doi:10.1029/2008JC005132.

LeVeque, J and D. L. George (2007): High-resolution finite volume methods for the shallow water equations with bathymetry and dry states. In P. L-F. Liu, H. Yeh, and C. Synolakis, editors, Advanced Numerical Models for Simulating Tsunami Waves and Runup, volume 10, pp 43-73. http://www.amath.washington.edu/ rjl/pubs/catalina04/.

LeVeque, R. J., D. L. George, and M. J. Berger (2011): Tsunami modeling with adaptively refined finite volume methods. Acta Numerica, pp 211-289.

Love, M R, D Z Friday, P R Grothe, K S Carignan, B W Eakins, and L A Taylor. 2012. "Digital Elevation Model of Astoria, Oregon: Procedures, Data Sources and Analysis" (June 22): 1–34.

NTHMP (National Tsunami Hazard Mitigation Program) (2012): Proceedings and Results of the 2011 NTHMP Model Benchmarking Workshop. Boulder: U.S. Department of Commerce/NOAA/NTHMP (NOAA Special Report) 436 pp.

Petersen, M. D., C. H. Cramer, and A. D. Frankel (2002): Simulations of Seismic Hazard for the Pacific Northwest of the United States from Earthquakes Associated with the Cascadia Subduction Zone. Pure Appl. Geophys., 159, 2147-2168.

Project Safe Haven (2011a): Vertical Evacuation on the Washington coast, Pacific County, Washington. Available at https://catalyst.uw.edu/workspace/wiserjc/19587/116498 .

Project Safe Haven (2011b): Vertical Evacuation Structures Conceptual Cost Analysis. Available at https://catalyst.uw.edu/workspace/wiserjc/19587/116498 .

Satake, Kenji, Kelin Wang and Brian F Atwater (2003): Fault Slip and Seismic Moment of the 1700 Cascadia Earthquake Inferred From Japanese Tsunami Descriptions, *Journal of Geophysical Research* 108 (B11): 1–17. doi:10.1029/2003JB002521.

TPSWG (2006): Seaside, Oregon Tsunami Pilot Study— Modernization of FEMA Flood Hazard Maps." *Joint NOAA/USGS/FEMA Report* (November 2): 1–176.

DOGAMI (2010): LIDAR Remote Sensing Data Collection, Southwest Washington. Submitted by Watershed Sciences. May 24, 2010.

Witter, Robert C, Yinglong Zhang, Kelin Wang, George R Priest, Chris Goldfinger, Laura L Stimely, John T English, and Paul A Ferro (2011): Simulating Tsunami Inundation at Bandon, Coos County, Oregon, Using Hypothetical Cascadia and Alaska Earthquake Scenarios. *DOGAMI Special Paper 43* (July 11): 1–63.